

Combined Effect of Isophthalic Acid and Polyethylene Glycol in Polyethylene Terephthalate Polymer on Thermal, Mechanical, and Gas Transport Properties

T. P. Mohan,¹ A. Prem George,² K. Kanny¹

¹*Polymer and Polymer Composites Research Group, Department of Mechanical Engineering, Durban University of Technology, Durban, South Africa*

²*Futura Polyesters Limited (Formerly Indian Organic Chemicals Limited), Chennai, Tamil Nadu, India*

Received 2 August 2010; accepted 13 January 2012

DOI 10.1002/app.36818

Published online in Wiley Online Library (wileyonlinelibrary.com).

ABSTRACT: The objective of this article is to study the combined effect of isophthalic acid (IPA) and polyethylene glycol (PEG-400) in PET polymer and film on thermal, mechanical, and gas transport properties. The purpose of developing this material is to reduce the melting point, improve mechanical, thermal, and gas barrier properties. The chosen raw materials, namely, IPA and PEG for copolyester synthesis will replace partially the acid and diol monomers of PET. The molar concentration of comonomers (IPA and PEG-400) were varied from 2 to 50% and

the result shows that the gas barrier properties (namely O₂, CO₂, N₂, and water vapor transmission rate), mechanical, and thermal properties were lesser than that of PET polymer. On improving the crystallinity of PET-isophthalate-PEG (PET-IP) copolymer, barrier properties are improved than that of PET polymer. © 2012 Wiley Periodicals, Inc. *J Appl Polym Sci* 000: 000–000, 2012

Key words: polyesters; mechanical properties; thermal barrier properties

INTRODUCTION

Polyethylene terephthalate (PET) is a thermoplastic polyester polymer produced by the reaction of monoethylene glycol (MEG) and terephthalic acid (PTA). Sometimes, dimethyl terephthalate is also used for PET production instead of PTA. PET polymer has superior strength, stiffness, chemical, heat resistance, and electrical properties. Production of PET polymer involves esterification of glycol and acid monomers followed by polymerization. Catalyst and accelerators are added during esterification and polymerization reactions to have effective reaction. After polymerization process of PET polymer, their molecular structure is generally amorphous with low-molecular weight (or molecular chain length). The crystallinity of the PET polymer can be improved by crystallizing at elevated temperature range above or at around crystallization temperature (T_{ch}). The properties of PET may vary based on its molecular weight, which is usually expressed by a parameter commonly called as intrinsic viscosity (IV). The more the chain length, the more will be

chain entanglements, which result in increased IV (molecular weight). The molecular weight (or chain length or IV) of the PET polymer can be increased by means of solid state polymerization (SSP) or the term also called as polycondensation.^{1–4} In general, PET can be processed into end products by injection molding, stretch blow molding, thermoforming, or extrusion. Depending on its processing and thermal history, PET may exist as an amorphous (transparent) or as a semicrystalline material. The semicrystalline material might appear transparent (spherulites <500 nm) or opaque and white (spherulites up to a size of micrometer) depending on its crystal structure and spherulite size.^{5–8}

Majority of PET polymers are used in food packaging, carbonated soft drink containers, and textile fiber industries, which requires high-gas barrier and mechanical properties.^{9–14} In these applications, a few amounts of comonomer are generally added during PET synthesis to induce clarity, improve properties or to enhance processing ability. Commonly used monomers for replacement in PET polymer are either acid or diol monomers. Replacement for acid monomer is fatty acids, isophthalic acids (IPAs), phthalates, other aliphatic/aromatic acids, etc., and diol monomer is cyclohexane dimethanol (CHDM), polyethylene glycol (PEG), etc.^{15–17} Replacing PTA with IPA creates a kink in the PET polymer chain. This interferes with crystallization by affecting the periodicity of molecular structure and thereby

Correspondence to: K. Kanny (kannyk@dut.ac.za).

Contract grant sponsor: National Research Foundation (NRF) of South Africa; contract grant number: 71599.

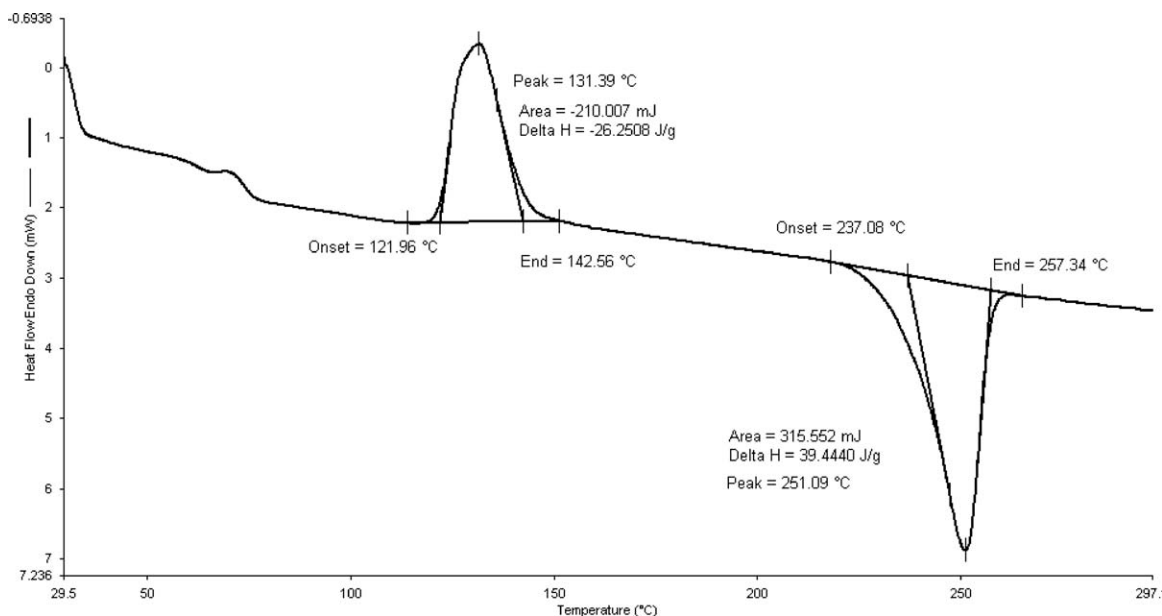


Figure 1 Heat 1 DSC scan of PET.

lowers the polymer's melting point.^{18–23} In some cases, for example, CHDM are also added to the polymer backbone in place of MEG. Since this building block of CHDM is much larger (six additional carbon atoms) than the ethylene glycol unit it replaces, it does not fit in with the neighboring chains the way an ethylene glycol unit would. This interferes with crystallization and lowers the polymer's melting temperature.^{24–26} Replacement of MEG with PEG in PET polymer is also reported in the literature, and this copolymer is extensively used in biomaterial applications.^{27–29} Literature on PET-PEG with improved shape memory effect and dynamic

mechanical properties due to the addition of cross-linking additives is available.^{30–33} Cationic dyeable salt additive on enhancing the dyeable properties in PET-PEG copolymer is observed by Hsiao et al.³⁴

The aim of this work is to study the combined effect of acid and diol replacement monomers on gas barrier, thermal, and mechanical properties of PET polymer. For carrying out this study, acid and diol monomers, namely, IPA and PEG-400 are planned for replacement in PTA and MEG monomer during the synthesis of PET polymer. Almost no work is reported on the combined effect of the IPA and PEG together in PET. In this work, the molar

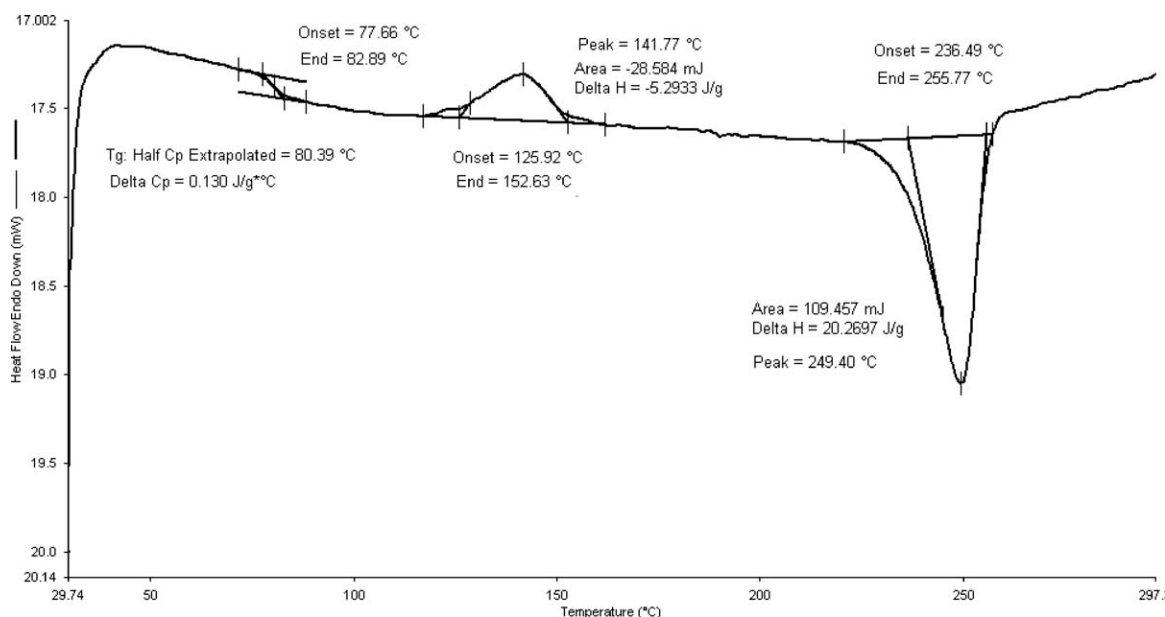


Figure 2 Heat 2 DSC scan of PET.

TABLE I
Thermal Properties of Crystalline PET and PET-IP Copolymer

% of IPA-PEG	IV (dL/g)	T_g (°C)	T_{ch} (°C)	T_m (°C)	T_{m1} (°C)	$\Delta H T_{m1}$ (J/g)	% Cryst.
Nil	0.811	80.39	141.77	249.4	251.1	43.2	34.30
2.0	0.810	79.51	152.6	247.9	236.6	41.6	33.04
4.0	0.806	78.81	163.1	239.7	237.7	40.1	31.80
6.0	0.800	77.03	159.5	232.8	224.4	38.6	30.70
8.0	0.809	77.93	173.4	225.8	230.3	37.5	29.80
9.0	0.804	75.81	176.7	222.1	226.7	37.1	29.30
10.0	0.808	74.63	177	222.5	234.8	36.1	28.70
12.0	0.807	74.13	177.3	216.6	221.5	35.3	28.00
25.0	0.801	72.41	163.1	198.1	203.3	32.7	26.01
40.0	0.813	70.30	151.1	155.3	158.3	26.5	21.12
50.0	0.798	68.11	143.7	150.3	153.1	22.8	18.11

concentration of comonomers concentration is varied from 2 to 50% in which each IPA and PEG monomer have equal contribution (50 : 50) in resultant PET polymer chain. The main objective of developing this material is to find an application in low melting PET polymer, improved thermal, mechanical, and gas barrier properties.

EXPERIMENTAL DETAILS

Raw materials

Test samples for this study are PET and PET-IP with various mole concentrations of IPA and PEG (2, 4, 6, 8, 9, 10, 12, 25, 40, and 50%) and were obtained from Futura Polyesters, India. The molar concentration of comonomers (IPA and PEG-400) in PET-IP represents combined addition of IPA and PEG-400 monomers. For example, PET-IP (50%) means the copolymer consists of 25 mole % IPA and 25 mole % PEG-400. All these samples were obtained in solid state polymerized forms.

Characterization

The SSP samples were kept in the oven at their respective crystallization temperature for specific time to obtain the desired crystallinity levels. Further, these different crystalline samples were used to perform gas barrier and mechanical properties measurements. IV is measured using Schott Gerate Obillo viscometer at 25°C, in which a 2.5 g of PET (or PET-IP) sample was dissolved in 25 mL of 50 : 50 ratio of CCl_4 : phenol solution. The thermal properties of PET and PET-IP system was measured by using DSC (Perkin Elmer-Pyris 6) at the scanning rate of 5°C/min from 30 to 285°C. Two heating scans were conducted in PET and PET-IP, Heat 1 scan to measure T_{m1} and Heat 2 to measure T_g (glass transition temperature), T_{ch} (crystallization temperature) and T_m (actual melting point of polymer). After taking the sample to 285°C in Heat 1, it is kept for a while and then quenched to room temperature to retain

the melt amorphous phase and then Heat 2 scan was carried out up to 285°C. The percent crystallinity was calculated based on the ratio of ΔH (J/g) of T_{m1} (test sample)/126 J/g (ΔH of 100% crystallized PET).³⁵ The gas barrier properties [CO_2 , O_2 , N_2 , and water vapor transmission rate (WVTR)] were measured from gas measuring system (GMS), Applied Films, Germany. Films of 3-mm thickness, length of 5 cm, and width of 5 cm were prepared and placed in the GMS system. O_2 , N_2 , and CO_2 gas pressure of 4 bar was applied at the one side of the film and kept for 3 days. The test was conducted in 78% atmosphere humidity condition. WVTR test was conducted as per ASTM F1249-06 standard conditions. The barrier properties of samples were measured in

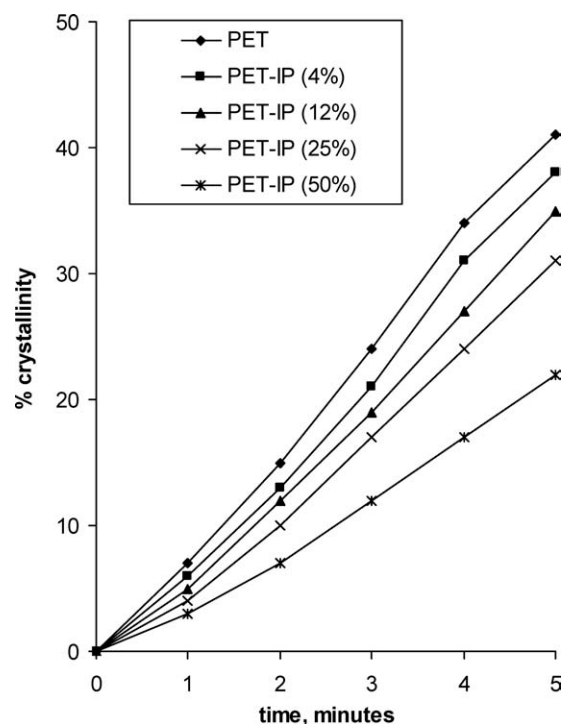


Figure 3 Rate of crystalline formation of PET and PET-IP series.

TABLE II
Gas Transport Properties of PET and PET-IPA Copolymer

Material	O ₂ cc.mil/100 in ² day atm, 30°C	CO ₂ cc.mil/100 in ² day atm, 30°C	N ₂ cc.mil/100 in ² day atm, 30°C	WVTR g.mil/100 in ² day, 30°C
PET	4.0	33	1.2	2.7
2%	8.8	48	2.3	3.7
4%	8.3	45	2.1	3.3
6%	8.1	42	1.9	3.5
10%	8.0	40	1.8	3.7
20%	6.5	35	1.7	3.3
50%	4.0	34	1.2	2.6

precrystallized condition (at constant IV condition), amorphous condition and 60% crystallized

For examining the mechanical properties, five injection-molded test specimens were made. PET, PET-IP, and PET-IP-nanoclay resins were predried at 160°C for 4 h before making test specimens. The molding temperature was kept at 135 and 260°C (hopper and nozzle), respectively. The barrel temperature was maintained at 205, 225, and 250°C across its length. Injection pressure of 1200 kg/cm³ and mold temperature was maintained at 80°C. Tensile and flexural properties were measured by Instron instrument using ASTM D638 and ASTM D790, respectively. Izod impact was measured using ASTM D256A. Heat deflection temperature (HDT) was measured using ASTM D648. Abrasion resistance was measured using ASTM D1044. The average value of the each result was considered. It was ensured that the values were within 3% standard deviation from the mean values. Wear surface of samples was observed using ZEISS AXIO LAB optical microscope. Elastic recovery properties of PET and PET-IP series were measured by using ASTM D6084 standard. Density and shore D hardness measurements were carried out using ASTM D1505-03 and ASTM D2240 methods for PET and PET-IP series, respectively.

RESULTS AND DISCUSSION

Thermal properties

Figures 1 and 2 show the Heat 1 and 2 DSC scan results of pure PET polymer, and Table I shows the DSC thermal properties of PET-IP series at constant IV condition. The results show that the melting point (T_m and T_{m1}) of PET continuously decreases as comonomers (IPA-PEG) content increases in PET polymer. Pure PET shows T_g of 80.39°C and for IPA-PEG copolymer series T_g values are within 2°C difference up to 4% IPA-PEG and above 4% IPA-PEG T_g starts decreasing rapidly. As reported elsewhere,¹⁵⁻³⁰ the reduction of T_g in PET is due to the kinking effect in the molecular structure, which arise due to the copolymer addition. The addition of comonomers in PET increases the T_{ch} temperature and suggests that the crystallization takes place at higher temperature. The melting point (T_m), T_g , and percent crystallinity of PET almost decreases linearly as IPA-PEG content increases in PET.

To study the crystalline behavior of PET and PET-IP series, the percent crystalline formation is measured at regular interval of time while keeping the samples at their respective T_{ch} temperature, and the result is shown in Figure 3. The result shows that the rate of formation of percent crystalline is higher

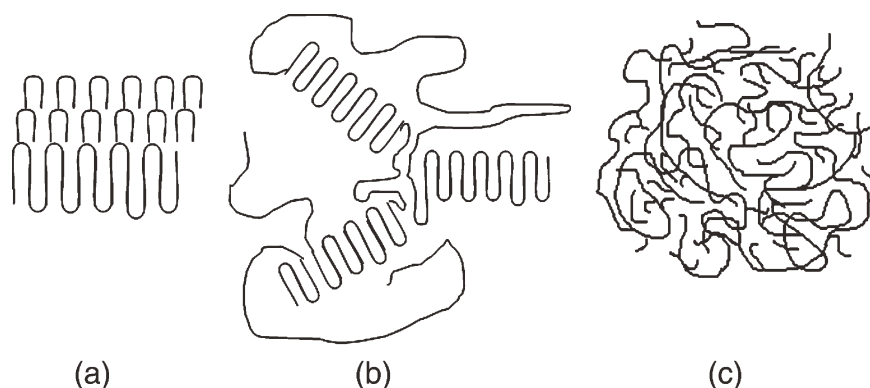


Figure 4 Schematic representation of molecular arrangement in (a) fully crystallized polymer, (b) semicrystalline polymer, and (c) amorphous polymer.

TABLE III
Gas Transport Properties of Amorphous PET-IP Series

PET-IP series	Density (g/cc)	O ₂ cc.mil/100 in ² day atm, 30°C	CO ₂ cc.mil/100 in ² day atm, 30°C	N ₂ cc.mil/100 in ² day atm, 30°C	WVTR g.mil/100 in ² day, 30°C
PET	1.2721	16	51	2.7	5.3
4%	1.2801	15	48	2.5	5.1
6%	1.2941	14	46	2.4	4.8
10%	1.2990	12	44	2.2	4.3
20%	1.3657	11	42	2.0	3.9
50%	1.3137	8	39	1.6	3.1

in PET polymer when compared with PET-IP series. The rate of crystalline formation continuously decreases when the IP content continuously increases in PET polymer. The possible reason for low-crystallization rate in PET-IP series is due to the presence of large molecular weight polymer backbone due to PEG-400. The PEG-400 is a high-molecular weight (~ 400 g/mole) when compared with ethylene glycol (~ 62 g/mole) and the replacement of low-molecular weight ethylene glycol by high-molecular weight PEG-400 in PET might have caused the bulky side group in PET and hence hinders the rate of rate of crystalline formation. Also, isophthalic acid present in PET-IP copolymer series in the place of terephthalic acid could affect the molecular periodicity in PET-IP copolymer and also hinders the crystallization.

Gas transport properties of PET and PET-IP films

The result of O₂, CO₂, N₂, and WVTR is shown in Table II. The barrier properties of PET polymer are better than that of PET-IP copolymers. However, the gas barrier property of PET-IP (50%) copolymer is almost at the same level to that of PET polymer. Even though the percent crystallinity of this copolymer (50% IP) is lower than that of PET polymer, the amorphous molecules could have formed a clustered molecular arrangement as reported elsewhere^{36–38} and could have reduced the gas permeation. To understand the gas permeation in the polymer molecules, Figure 4 shows the schematic arrangement of

various types of molecular structures. Fully crystallized polymer shows well-improved gas barrier properties due to the periodic arrangement of molecules. In semicrystalline polymers, the permeation of gas molecules takes place via the amorphous molecules and hence shows the reduced gas barrier properties than fully crystalline polymer. In amorphous molecules, the gas permeation will be higher due to the random arrangement of polymer molecules. This random arrangement of polymer molecules causes intermolecular void or space and hence facilitates easy transport of gas molecules.

As discussed elsewhere,^{36–38} the clustered arrangement of molecular phenomenon is used to explain the permeation of molecules in amorphous molecules. In the clustered molecular arrangement, the permeation of gas molecules in amorphous polymers depends on various factors, namely, intermolecular space (or void), their size, shape, density, microscale voids of amorphous molecules, etc. The lower the intermolecular space in amorphous molecules, the lower will be the gas permeation. In the PET-IP copolymer, the presence of clustered arrangement of amorphous molecules with low-intermolecular void space can be supported to some extent because of their increased density and understanding their molecular structure. The net molecular weight in PET-IP series is higher than that of PET polymer due to the presence of higher molecular weight PEG-400. The increased molecular weight of PEG-400 causes the increased density of PET-IP series than that of PET polymer (Table V). Also the molecular size of

TABLE IV
Gas Transport Properties of Higher Crystallinity Content (60%) of PET-IP Series

PET-IP series	O ₂ cc.mil/100 in ² day atm, 30°C	CO ₂ cc.mil/100 in ² day atm, 30°C	N ₂ cc.mil/100 in ² day atm, 30°C	WVTR g.mil/100 in ² day, 30°C
PET	3.7	30	1.1	1.9
4%	3.7	29	1.2	1.9
6%	3.7	27	1.1	1.9
10%	3.7	24	1.1	1.8
20%	3.6	20	0.9	1.7

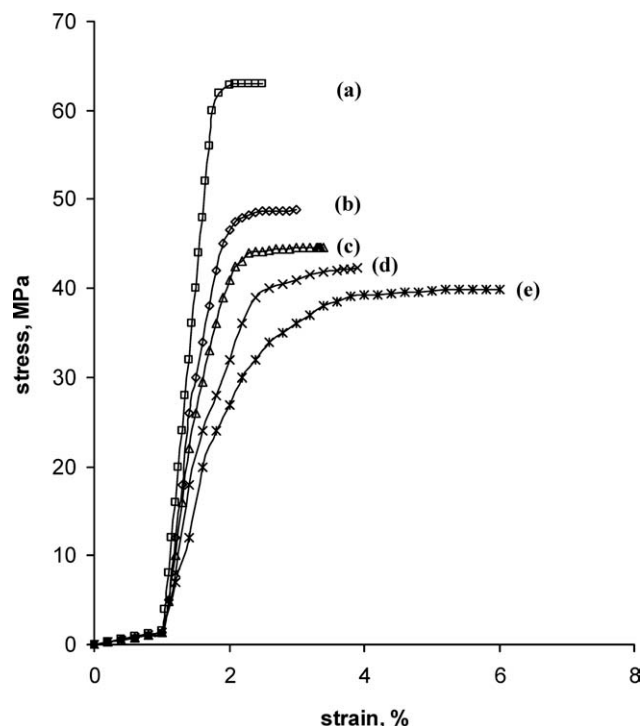


Figure 5 Tensile stress–strain curves of (a) PET, (b) PET-IP (4%), (c) PET-IP (12%), (d) PET-IP (25%), and (e) PET-IP (50%).

PEG-400 is more than that of ethylene glycol and this could have possibly reduced the void space of amorphous molecules, and this effect is predominantly observed in higher IP content (50%). To substantiate the clustering effect of amorphous molecules and their permeation, it is decided to study the permeation properties of amorphous PET and PET-IP series. Table III shows the gas barrier properties of PET and PET-IP series for almost 100% amorphous sample. The amorphous samples are produced by rapidly quenching the sample to room temperature from the molten state. The result shows that the gas barrier properties for all PET-IP series are better than that of amorphous PET sample. The permeation property continuously increases in PET-IP series as IP content continuously increases in PET

polymer. Among the amorphous samples, PET shows low density than PET-IP copolymer series. The lower permeation in fully amorphous PET-IP copolymer is due to the clustered arrangement of amorphous molecules.

Although there exists crystalline phase in other PET-IP copolymer series, the gas permeation is more than that of PET polymer. The possible reason for low-barrier properties in PET-IP copolymers series (other than PET-IP 50) may be due to the insufficient crystallinity or less amount of clustering of amorphous molecules. To overcome this effect in PET-IP series and to improve gas barrier properties, it is decided to increase the percent crystallinity. Hence PET-IP copolymers were heated at their respective crystallization temperature (T_{ch}) for various time periods (15 min to 1 h). When the permeation were examined, it shows an improved barrier properties in PET-IP series and the barrier properties are comparable with that of even 60% crystallized pure PET (Table IV). In the 60% crystallized PET polymer, even though barrier properties are improved than that of precrystallized polymer due to increased percent crystallinity, the rate of increase of barrier properties is lower than that of PET-IP copolymer series. The remaining amorphous zones ($\sim 40\%$) in PET does not induced much clustering effect as observed in PET-IP series.

Mechanical properties of PET and PET-IP copolymers

Figure 5 shows the tensile stress–strain curves of PET and PET-IP series. It shows that the tensile characteristics of PET-IP copolymers are different from that of pure PET polymer. The strength and modulus were continuously decreased as IPA-PEG content continuously increase in PET polymer. However, strain at failure increases as comonomers content increases in PET. The other mechanical properties of PET and PET-IP series are shown in Table V. IPA-PEG addition in PET reduces the HDT and Flexural strength. Negligible effect in the

TABLE V
Mechanical Properties of PET and PET-IP Series at 0.8 IV Condition

Properties	Unit	PET	PET-IP (4%)	PET-IP (12%)	PET-IP (25%)	PET-IP (50%)
Tensile strength	MPa	63.04	48.78	44.56	42.32	39.87
Tensile modulus	GPa	1.48	1.39	1.33	1.316	1.301
Elongation at break	%	2.5	3.1	3.4	3.9	6
HDT	°C	67.5	66.3	65.4	64.8	63.9
Density	g/cc	1.3452	1.3457	1.3513	1.3561	1.3593
Flexural strength	MPa	78.6	71.6	64	54.2	47.8
Flexural modulus	MPa	1.6	2	2.1	2.3	2.6
Izod impact	J/m	11.29	13.6	25.5	32.2	47.8
Shore D	–	54.1	53.3	52.4	51.8	51.1
Abrasion resistance	mg/1000 cycle	60	50	45	35	25

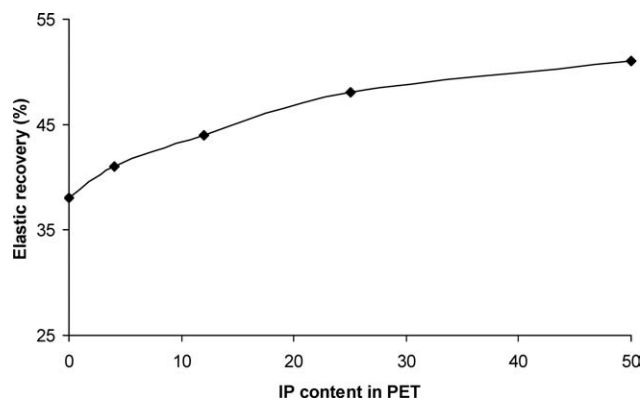


Figure 6 Effect of IP content on elastic recovery of PET.

density and hardness of the PET and PET-IP series was observed. Improved flexural modulus, impact strength, and abrasion resistance was observed on addition of IPA-PEG in PET polymer. Figure 6 shows the elastic recovery properties of PET and PET-IP series. The result shows that the PET-IP copolymer shows improved elastic recovery properties than that of PET polymer. The elastic recovery continuously increases in PET polymer when IP content

continuously increases suggesting that the elastic rebound characteristics are better in these PET-IP polymers series.

The cause of low-abrasion resistance in PET was studied by viewing wear surface of tested specimen. Figure 7 shows the optical microscope of wear surface of PET and PET-IP (40%). The wear surface of PET shows some deep ploughing marks, whereas PET-IP 40% shows the absence of such marking. The mode of material removal is by the ploughing action of the hard wear disk. The hard disk removes the material as wear debris, and this resulted in high-material loss in PET polymer.

Table VI shows the mechanical properties of 60% crystallized PET-IP series. Because of the increase of crystallinity in PET-IP series, improvement in tensile modulus, HDT, density, and hardness properties are observed. Also, the other mechanical properties were relatively unaffected. Another important observation is that the melting point of PET-IP series is lower than that of PET polymer and also shows improved mechanical properties. This suggests that the PET-IP series can be processed at lower temperature than that of PET polymer.

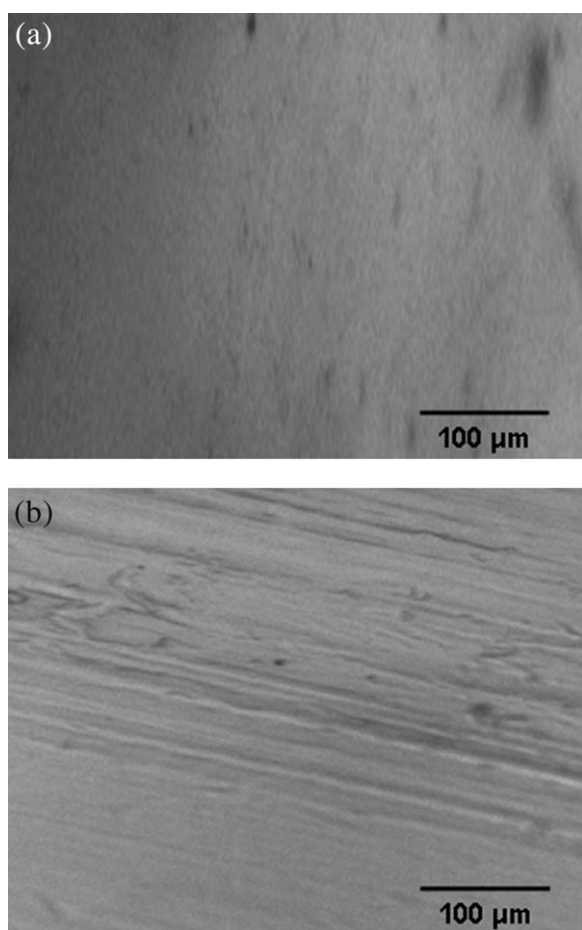


Figure 7 Wear surface of (a) PET-IP (40%) and (b) PET.

Mechanical properties of PET and PET-IP copolymer films

Table VII shows the mechanical properties of 60% crystallized PET and PET-IP based films. The result shows improved tensile modulus and elongation at break values for PET and PET-IP series. The stretching processes in the films have caused an improvement in modulus and strain values at break values. The molecules are orderly oriented in the stretching direction and results in improved modulus and strain values. Moreover, there is a slight increase in crystallinity of stretched films when compared with the crystallinity of raw chips (60%). This increase in crystallinity is attributed due to the stretching and orientation of molecules.

TABLE VI
Mechanical Properties of 60% Crystallized PET-IP Series

Properties	Unit	PET	PET-IP (4%)	PET-IP (12%)
Tensile strength	MPa	63.04	49.1	45.3
Tensile modulus	GPa	1.48	1.79	1.66
Elongation at break	%	2.5	3.0	3.3
HDT	°C	67.5	71	69.7
Density	g/cc	1.3452	1.372	1.386
Flexural strength	MPa	78.6	72.3	63.7
Flexural modulus	MPa	1.6	2.3	2.8
Izod impact	J/m	11.29	14	24
Shore D hardness	–	55	54.3	53.8
Abrasion resistance	mg/1000 cycle	60	51	47

TABLE VII
Mechanical Properties of 60% Crystallized PET and PET-IP Films

Properties	Tensile strength (MPa)	Tensile modulus (GPa)	Elongation at break (%)	Density (g/cc)	% Crystallinity
PET	63.0	1.61	2.71	1.3461	63
PET-IP (4%)	51.7	1.83	3.2	1.3703	66
PET-IP (12%)	47.3	1.71	3.3	1.3912	64

CONCLUSIONS

A new class of PET-based copolymer consisting of acid and diol replacement monomer namely IPA and PEG were developed, and the comonomers effect on thermal, mechanical, and gas transport properties of PET has been studied in this work. Following conclusions are drawn.

1. At constant IV conditions (0.8 dL/g), the T_m , T_g , and crystallinity of PET continuously decreases when IPA-PEG content continuously increases in PET.
2. The O_2 , CO_2 , N_2 , and WVTR tests shows reduced barrier properties in PET-IP precrystallized samples, except for PET-IP (50%). On crystallizing PET-IP copolymers, improved barrier properties are observed. The threshold level of 60% crystallinity in PET-IP is required to achieve comparable or improved gas barrier properties. The amorphous samples show improved gas barrier properties in PET-IP series than that of PET polymer.
3. The addition of IPA-PEG in PET decreases the tensile strength, tensile modulus, flexural strength, HDT, and Rockwell hardness. On the other hand, addition of IPA-PEG in PET increases tensile elongation at break, flexural modulus, impact strength, abrasion resistance, and elastic recovery properties. Negligible effect in hardness and density of PET is observed when filled with IPA-PEG monomers. On improving the crystallinity of PET-IP copolymer, improvement in tensile modulus, HDT, density, impact, and hardness properties are observed. Improved mechanical properties are also observed in the stretched films.

References

1. Ravindranath, K.; Mashelkar, R. A. *Chem Eng Sci* 1986, 4, 2197.
2. Ershad-Langroudi, A.; Jafarzadeh-Dogouri, F.; Razavi-Nouri, M.; Oromiehie, A. *J Appl Polym Sci* 2008, 110, 1979.
3. Reinsch, V. E.; Rebenfeld, L. *J Appl Polym Sci* 2003, 52, 649.
4. Rezaeian, I.; Jafari, S. H.; Zahedi, P.; Nouri, S. *Polym Compos* 2009, 30, 993.
5. Jabarin, S. A. *Polym Eng Sci* 1991, 31, 1071.
6. Gueguen, O.; Ahzi, S.; Makradi, A.; Belouettar, S. *Mech Mater* 2010, 42, 1.
7. Arnoult, M.; Dargent, E.; Mano, J.F. *Polymer* 2007, 48, 1012.
8. Awaja, F.; Pavel, D. *Eur Polym J* 2005, 41, 1453.
9. Motta, O.; Di Maio, L.; Incarnato, L.; Acierno, D. *Polymer* 1996, 37, 2373.
10. Langevin, D.; Grenet, J.; Saiter, J. M. *Eur Polym J* 1994, 30, 339.
11. Shields, R. J.; Bhattacharyya, D.; Fakirov, S. *Compos A: Appl Sci Manuf* 2008, 39, 940.
12. Ozen, I.; Bozoklu, G.; Dalgiçdir, C.; Yucel, O.; Unsal, E.; Çakmak, M.; Menciloglu, Y. Z. *Eur Polym J* 2010, 46, 226.
13. Hu, Y. S.; Prattipati, V.; Mehta, S.; Schiraldi, D. A.; Hiltner, A.; Baer, E. *Polymer* 2005, 46, 2685.
14. Lange, J.; Wyser, Y. *Packag Technol Sci* 2003, 16, 149.
15. Wang, L.; Xie, Z.; Bi, X.; Wang, X.; Zhang, A.; Chen, Z.; Zhou, J.; Feng, Z. *Polym Degrad Stab* 2006, 91, 2220.
16. Wang, L. C.; Chen, J. W.; Liu, H. L.; Chen, Z. Q.; Zhang, Y. *Polym Int* 2004, 53, 2145.
17. Zhang, Y.; Feng, Z. G.; Zhang, A. Y. *Polym Int* 2003, 52, 1351.
18. Sakar, D.; Cankurtaran, O.; Karaman, F. Y. *J Appl Polym Sci* 2005, 98, 2365.
19. Higashi, F.; Takakura, T.; Sumi, Y. *J Polym Sci Part A: Polym Chem* 2004, 42, 2321.
20. Kotek, R.; Pang, K.; Schmidt, B.; Tonelli, A. *J Polym Sci Part B: Polym Phys* 2004, 42, 4247.
21. Li, X.; Liu, R.; Zhong, L.; Gu, L. *J Appl Polym Sci* 2003, 89, 1696.
22. Karayannidis, G. P.; Bikiaris, D. N.; Papageorgiou, G. Z.; Pas-tras, S. V. *J Appl Polym Sci* 2002, 86, 1931.
23. Schiraldi, D. A.; Gould, S. A. C.; Occelli, M. L. *J Appl Polym Sci* 2001, 80, 750.
24. Tsai, Y.; Fan, C.-H.; Hung, C.-Y.; Tsai, F.-J. *J Appl Polym Sci* 2007, 104, 279.
25. Sepehri, S.; Rafizadeh, M.; Afshar-Taromi, F. *J Appl Polym Sci* 2009, 113, 3520.
26. Quintana, R.; de Ilarduya, A. M.; Guerra, S. M.; Fernández, M.; Muñoz, M. E.; Santamaría, A. *Macromol Mater Eng* 2008, 293, 836.
27. Qian, Z.; Li, S.; He, Y.; Liu, X. B. *Polym Degrad Stab* 2004, 83, 93.
28. Barcellos, I. O.; Carobrez, S. G.; Pires, A. T. N.; Alvarez-Silva, M. *Biomaterials* 1998, 19, 2075.
29. Deschamps, A. A.; van Apeldoorn, A. A.; Heyence, H.; de Bruijn, J. D.; Karst, U.; Gripmaa, D. W.; Feijen, J. *Biomaterials* 2004, 25, 247.
30. Chung, Y.-C.; Shim, Y. S.; Chun, B. C. *J Appl Polym Sci* 2008, 109, 3533.
31. Park, C.; Lee, J. Y.; Chun, B. C.; Chung, Y.-C.; Cho, J. W.; Cho, B. G. *J Appl Polym Sci* 2004, 94, 308.
32. Chun, B. C.; Cha, S. H.; Park, C.; Chung, Y.-C.; Park, M. J.; Cho, J. W. *J Appl Polym Sci* 2003, 90, 3141.
33. Chun, B. C.; Cha, S. H.; Chung, Y.-C.; Cho, J. W. *J Appl Polym Sci* 2002, 83, 27.
34. Hsiao, K.-J.; Kuo, J.-L.; Tang, J.-W.; Chen, L.-T. *J Appl Polym Sci* 2005, 98, 550.
35. Christel, A.; Culbert, B. A.; Jurgens, T. U.S. Pat. 0,225,471 (2007).
36. Ugrozov, V. V. *Colloid J* 2010, 72, 574.
37. Devallencourt, C.; Marais, S.; Saiter, J. M.; Labbe, M.; Matayer, M. *Polym Test* 2002, 21, 253.
38. Jansen, J. C.; Friess, K.; Drioli, E. *J Membr Sci* 2001, 367, 141.